



DIGITAL ACCESS TO SCHOLARSHIP AT HARVARD

Characterization of the RpoN Regulon Reveals Differential Regulation of T6SS and New Flagellar Operons in *Vibrio cholerae* O37 Strain V52

The Harvard community has made this article openly available. [Please share](#) how this access benefits you. Your story matters.

Citation	Dong, Tao G., and John J. Mekalanos. 2012. Characterization of the RpoN regulon reveals differential regulation of T6SS and new flagellar operons in <i>Vibrio cholerae</i> O37 strain V52. <i>Nucleic Acids Research</i> 40(16): 7766-7775.
Published Version	doi:10.1093/nar/gks567
Accessed	February 19, 2015 10:50:09 AM EST
Citable Link	http://nrs.harvard.edu/urn-3:HUL.InstRepos:10536040
Terms of Use	This article was downloaded from Harvard University's DASH repository, and is made available under the terms and conditions applicable to Other Posted Material, as set forth at http://nrs.harvard.edu/urn-3:HUL.InstRepos:dash.current.terms-of-use#LAA

(Article begins on next page)

Characterization of the RpoN regulon reveals differential regulation of T6SS and new flagellar operons in *Vibrio cholerae* O37 strain V52

Tao G. Dong and John J. Mekalanos*

Department of Microbiology and Immunobiology, Harvard Medical School, 200 Longwood Avenue, Boston, MA 02115, USA

Received March 16, 2012; Revised May 1, 2012; Accepted May 18, 2012

ABSTRACT

The alternative sigma factor RpoN is an essential colonization factor of *Vibrio cholerae* and controls important cellular functions including motility and type VI secretion (T6SS). The RpoN regulon has yet to be clearly defined in T6SS-active *V. cholerae* isolates, which use T6SS to target both bacterial competitors and eukaryotic cells. We hypothesize that T6SS-dependent secreted effectors are co-regulated by RpoN. To systemically identify RpoN-controlled genes, we used chromatin immunoprecipitation coupled with sequencing (ChIP-Seq) and transcriptome analysis (RNA-Seq) to determine RpoN-binding sites and RpoN-controlled gene expression. There were 68 RpoN-binding sites and 82 operons positively controlled by RpoN, among which 37 operons had ChIP-identified binding sites. A consensus RpoN-binding motif was identified with a highly conserved thymine (–14) and an AT-rich region in the middle between the hallmark RpoN-recognized motif GG(–24)/GC(–12). There were seven new RpoN-dependent promoters in the flagellar regions. We identified a small RNA, *flaX*, downstream of the major flagellin gene *flaA*. Mutation of *flaX* substantially reduced motility. In contrast to previous results, we report that RpoN positively regulates the expression of *hcp* operons and *vgrG3* that encode T6SS secreted proteins but has no effect on the expression of the main T6SS cluster encoding sheath and other structural components.

INTRODUCTION

Cholera is a serious threat to public health in the developing countries. The cholera outbreak in Haiti has resulted in >6000 deaths and about a half-million confirmed

cases (1). As the causative pathogen for cholera, *Vibrio cholerae* has many virulence factors including cholera toxin, the critical colonization factor TCP pili, and virulence regulators ToxR and ToxT [reviewed in (2)]. A newly identified protein secretion system, Type VI secretion system (T6SS), has also been implicated in the virulence of *V. cholerae* by causing cytotoxicity in macrophage and inducing intestinal inflammation (3–5).

T6SS is a conserved protein delivery system present in >100 Gram-negative bacterial species including many important pathogens, *V. cholerae* (5), *Pseudomonas aeruginosa* (6), *Burkholderia thailandensis* (7), *Serratia marcescens* (8) and avian pathogenic *Escherichia coli* (9). In *V. cholerae*, T6SS genes are organized in one large locus consisting of 17 genes encoding mostly basal components and two *hcp-vgrG* operons encoding secreted proteins (5) (Supplementary Figure S1). Structural analysis shows that T6SS components are highly similar to phage tail proteins (10,11). For example, the T6SS-secreted Hcp and VgrG proteins are homologous to the tail tube protein and spike-like protein of T4 phage, respectively (11). Expression of T6SS genes is regulated by quorum sensing, TsrA and RpoN (5,12,13).

RpoN is an alternative sigma factor that binds to the core RNA polymerase and directs gene expression from RpoN-recognized promoters (14). RpoN positively regulates the expression of 70 genes in *E. coli* K-12, including genes for motility and nitrogen assimilation (15). However, the RpoN regulon has not been clearly defined in *V. cholerae*. RpoN-mediated transcription requires an enhancer that activates transcription by binding to upstream regions (16). The T6SS locus encodes an RpoN-enhancer VasH that is required for Hcp secretion and T6SS function (17). RpoN is essential for colonization in *V. cholerae* O1 classical strain O395, and it controls motility and expression of glutamine synthetase GlnA (18). However, the colonization defect of the *rpoN* mutant is not because of loss of motility or GlnA expression, suggesting the involvement of other RpoN-controlled traits (18). Microarray profiling studies

*To whom correspondence should be addressed. Tel: +1 617 432 1935; Fax: +1 617 738 7664; Email: john_mekalanos@hms.harvard.edu

of the effect of *rpoN* mutation on rugosity (19) and motility (20) show the expression of a large number of genes is altered in *rpoN* mutants of *V. cholerae* O1 El Tor strain and serotype O1 classical strain O395, respectively. Interestingly, T6SS genes are up-regulated in the *rpoN* mutants of these strains (19,20). This difference in RpoN control of T6SS is likely because of strain variation, as T6SS is not active in the seventh pandemic *V. cholerae* O1 El Tor strain and O395 strain under laboratory conditions (5). In addition, heterologous expression of T6SS-promoter reporter fusions was shown to be RpoN-dependent (21), suggesting that the T6SS cluster and *hcp* operons are co-regulated by RpoN.

T6SS targets both eukaryotic hosts and prokaryotic competitors, although the mechanism is not fully understood. *Pseudomonas aeruginosa* T6SS secretes effector proteins that are toxic to *E. coli* by degrading peptidoglycan (22,23). T6SS of *V. cholerae* is also required for killing *E. coli* (24), but the effectors have not been clearly defined. The actin-crosslinking domain of VgrG1 is translocated into macrophage cells resulting in cytotoxicity (4,25), and a newly identified secreted factor VasX is important for T6SS-mediated virulence in the model amoeba *Dictyostelium discoideum* (26).

In this study, our primary interest is to fully understand the regulatory role of RpoN in T6SS secretion and other cellular functions in *V. cholerae*. Chromatin-immunoprecipitation coupled with next-generation sequencing, ChIP-Seq, provides a powerful tool to identify protein-DNA interactions. ChIP-Seq has been mostly used in eukaryotic systems and there are few reports in bacteria. Our lab previously demonstrated the effectiveness of ChIP-Seq in bacterial studies and identified the Fur regulon in *V. cholerae* (27). Here we used the same approach combined with RNA-Seq to characterize the RpoN regulon in a T6SS-active, serotype O37 clinical isolate V52. There were 37 operons that show RpoN-dependent expression and RpoN-binding sites, indicative of direct control by RpoN. We uncovered new RpoN-controlled promoters in the flagellar gene clusters, and a small RNA that is important for motility. In addition, RpoN was found to selectively control the expression of T6SS secreted proteins but not the structural components.

MATERIALS AND METHODS

Bacterial strains and growth conditions

Strains and plasmids are listed in Table 1. A serotype O37 clinical isolate of *V. cholerae* strain V52 was used in this study. *Escherichia coli* DH5 α and SM10 λ pir were used for cloning and conjugation, respectively. Antibiotics were used at the following concentrations: ampicillin (100 μ g/ml), streptomycin (100 μ g/ml), kanamycin (50 μ g/ml) and chloramphenicol (2.5 μ g/ml for *V. cholerae* and 25 μ g/ml for *E. coli*). Arabinose (0.1%) was used for induction, unless otherwise specified. Motility was tested on Luria Bertani (LB) medium with 0.3% agar.

All strains were routinely grown at 37°C in LB medium containing 5 g/l sodium chloride. For ChIP- and RNA-Seq analyses, cultures were grown in LB medium to exponential phase (OD₆₀₀ = 0.5) and induced with 0.1% arabinose for 30 minutes at 37°C.

DNA manipulation

In-frame gene deletion in *V. cholerae* was performed as described (28,29). Briefly, the flanking region of the respective gene was amplified by crossover PCR, cloned into the pWM91 suicide vector, and transferred into recipient strains through conjugation. Independent transconjugants were purified and incubated on 5% sucrose to select for sucrose-resistant segregants. Deletion was confirmed by sequencing. For gene induction, the respective gene was PCR-amplified, digested with KpnI and Sall, and cloned into the pBAD18 plasmid (31) carrying a C-terminal 3xV5 epitope tag (32). The small RNA *flaX* was cloned into a plasmid pNM12, a pBAD24-derivative vector that lacks ribosomal binding sites upstream of the cloning site and is commonly used for expressing sRNAs (30). All constructs were verified by sequencing. Primers used in this study are listed in Supplementary Table S1.

Western blot

Proteins were resolved in a precast 10% SDS PAGE gel (Life Technologies) and transferred to a PVDF membrane (Millipore) by electrophoresis. The membrane was then blocked in 5% non-fat milk for 1 hour at room temperature, and incubated with respective monoclonal antibodies at 4°C overnight. The monoclonal antibodies to V5-tag,

Table 1. Strains and plasmids used in this study

Strain and plasmid	Genotype or phenotype	Reference
<i>V. cholerae</i>		
V52	Serotype 37 clinical isolate from Sudan	Pukatzki <i>et al.</i> , 2006 (5)
V52 <i>rpoN</i>	Knock-out <i>rpoN</i> mutant of V52	This study
T6SS mutants	Nonpolar deletion mutants of V52	Zheng <i>et al.</i> , 2010 (12)
SM10	<i>thi thr leu tonA lac Y supE recA::RP4-2-Tc::Mu</i>	Miller and Mekalanos, 1988 (28)
Plasmid		
pWM91	Suicidal conjugation vector	Metcalf <i>et al.</i> , 1996 (29)
pBAD18V5	Expression vector with 3xV5 tag	Davies <i>et al.</i> , 2011 (27)
pRpoN	The <i>rpoN</i> gene cloned into pBAD18V5	This study
pNM12	sRNA expression vector derivative of pBAD24	Majdalani <i>et al.</i> , 1998 (30)
pflaX	<i>flaX</i> inserted between NheI and KpnI sites on pNM12	This study

RpoB and T6SS components were from Sigma Aldrich, NeoClone and laboratory stock, respectively. The membrane was then washed three times in TBST buffer (50 mM Tris, 150 mM NaCl, 0.05% Tween-20, pH 7.6) and incubated with a HRP-conjugated secondary antibody (Pierce) for 1 hour at room temperature. Signals were detected using the ECL solution and ECL films (Amersham). Western blotting was performed at least twice for each experiment.

Protein secretion assay

Cultures were grown in LB medium to exponential phase ($OD_{600} = 0.5$). Expression was induced by 0.1% L-arabinose for 1 hour. One millilitre culture was centrifuged twice at $20\,000 \times g$ for 2 minutes, and the supernatant was then filtered through a 0.2- μ m filter. A mixture of 900 μ l of supernatant and 100 μ l of 100% TCA solution was placed on ice for 2 hours and centrifuged at $15\,000 \times g$ for 20 minutes at 4°C. The supernatant was discarded and the pellet was washed twice with 1 ml of 100% acetone by centrifugation at $20\,000 \times g$ for 5 minutes. The resultant pellet was mixed with 30 μ l of SDS-loading dye and proteins analyzed by western blot analysis.

Chromatin immunoprecipitation paired with next-generation sequencing ChIP-Seq

ChIP assay was performed as described previously (27). Briefly, 50 ml culture was mixed with formaldehyde (1% final concentration) for cross-linking at room temperature for 20 minutes, and the reaction was quenched by glycine (0.5 M). Cells were collected by centrifugation, washed twice with TBS buffer, and resuspended in 1 ml lysis buffer (10 mM Tris, 100 mM NaCl, 1 mM EDTA, 0.5 mM EGTA, 0.1% deoxycholate, 0.5% N-lauroylsarcosine, pH 8.0) with protease inhibitor cocktail (Sigma). Cells were then lysed with 1 mg/ml lysozyme at 37°C for 30 minutes and sonicated for 10 minutes using a cup horn sonicator at 60% power setting (Misonix). Cell debris was removed by centrifugation at $16\,000 \times g$ for 15 minutes at 4°C, and the supernatant containing DNA fragments with an average size of 200 bp was incubated with pretreated Dynal-Protein G beads coated with anti-V5 monoclonal antibody (Sigma). A control sample (100 μ l) was taken before Dynal-bead treatment. ChIP reaction was carried out at 4°C overnight on a rotary shaker, and samples were washed five times with RIPA buffer (50 mM HEPES buffer, 500 mM LiCl, 1 mM EDTA, 1% Nonidet P-40, 0.7% deoxycholate, pH 7.5) and once with TBS buffer. ChIP DNA was eluted in 100 μ l elution buffer (50 mM TE buffer, 1% EDTA, pH 7.5) at 65°C for 30 minutes and de-cross-linked by incubation at 65°C overnight. Samples were then treated with RNase A and proteinase K, and purified with a ChIP DNA clean kit (Zymo). Experiments were performed in triplicate.

RNA extraction

RNA was extracted from three independent replicates of exponential phase cultures using acidic phenol (pH 4.3, Sigma) and purified with a Direct-zol RNA kit (Zymo).

The quality of RNA was examined with Bioanalyzer (Agilent). Ten micrograms of total RNA was treated with an Ambion rRNA kit to remove ribosomal RNA, and the efficiency was confirmed by Bioanalyzer analysis.

Library construction and Illumina HiSeq sequencing

Libraries for ChIP-Seq and RNA-Seq were prepared using NEBNext® ChIP-Seq Sample Prep Master Mix Set 1 (NEB) and NEBNext® mRNA Sample Prep Master Mix kit (NEB), respectively. Briefly, ChIP DNA was end-repaired ligated to Illumina adaptors, and selected for a fragment size of around 200 bp by gel extraction. RNA samples were treated similarly, except for two additional steps of fragmentation and cDNA synthesis before end-repair. Multiplex Illumina primers were used to PCR-amplify gel-extracted products, and products were purified with a DNA clean-up kit (Zymo).

Sequencing was performed using an Illumina HiSeq2000 platform in the Biopolymer core facility at Harvard Medical School. ChIP-Seq and RNA-Seq reads were mapped to *V. cholerae* N16961 genome using the software CLC Genomics Workbench as previously described (27). ChIP-Seq and RNA-Seq data generated average genome coverage of 4-fold and 40-fold, respectively. Three independent ChIP samples were compared with the reference, and enriched peaks were detected by scanning the genome with a 120-bp sliding window. Identified peaks are ranked by the false discovery rate (FDR), which is estimated as previously describe (33). Genuine RpoN-binding sites are peaks identified in all three ChIP samples with a cut-off FDR value ($1E-26$) that corresponds to the highest FDR for previously known binding sites. Consensus RpoN-binding motif was generated by searching ChIP peak regions using the MEME Suite program (34). For RNA-Seq, gene expression level is represented as the RPKM value (reads per kilobase per million mapped reads) (35). We use a two-fold change in average gene expression and Student's t-test *P* value < 0.05 as criteria to identify RpoN-controlled genes. The average RPKM value for the *rpoN* gene was 345-fold higher in the *rpoN*-positive strain than in the *rpoN* mutant that had only background values, indicating a good quality of RNA-Seq data.

Quantitative PCR (qPCR)

To validate ChIP-Seq and RNA-Seq results, qPCR was performed using the Fast SYBR green mix (Kapa Biosystems). For transcriptional expression analysis, one-step qPCR was performed with the RNA-Ct one-step system (Applied Systems). The *rrsA* gene, encoding 16S RNA, was used as a control sample for normalization of difference in sample quantities.

Northern blot analysis

Total RNA (10 μ g) and ssRNA ladder (2 μ g) were mixed with ssRNA ladder loading buffer (NEB), respectively, and incubated at 75°C for 5 minutes and 4°C for 2 minutes. Samples were resolved on a 6% TBE-Urea gel (Life Technologies) at 150 V for 1 hour and transferred to a Hybond N membrane at 70 V for 2 hours. After

UV-cross-linking twice at 1200J, the membrane was pre-hybridized with ULTRAhyb[®]-Oligo buffer (Life Technologies) at 45°C for 30 minutes and then hybridized with 100 pmol of ³²P labeled probe overnight. The membrane was washed twice with 2 × SSC (saline-sodium citrate) buffer and exposed to film for 24 hours before development.

RESULTS

RpoN-recognized promoter regions identified by ChIP-Seq

As a transcription factor, the importance of RpoN in virulence and other functions results from the effects of its regulated genes. To characterize these genes and identify RpoN-binding promoters, we performed ChIP experiments in an *rpoN* knockout mutant expressing an epitope-tagged RpoN or the empty vector as a control subject. The C-terminus of RpoN was fused with a 3xV5 tag that has been shown with high ChIP efficiency in *V. cholerae* (27). To test whether this construct is functional, we examined two known RpoN-dependent traits, motility and Hcp expression. The *rpoN* mutant was complemented by the RpoN-3V5 construct for motility and expression of Hcp (Figure 1), indicative of a functional RpoN.

Using ChIP-Seq analysis, we found 68 RpoN-binding peaks common in three replicate samples (Figure 2, Supplementary Table S2). These peak-associated genes are involved in motility, T6SS secretion, nitrogen utilization, lipoprotein and membrane and unknown functions. By comparing all peak sequences, we identified a consensus 15 bp RpoN-binding motif, tGG(-24)cacnntttTGC(-12), capital letter indicating highly conserved sequences (Figure 2). Although it closely resembles the canonical RpoN-recognized sequence identified in *E. coli* (15), the RpoN-binding motif in *V. cholerae* differs from *E. coli* motif with a

more AT-rich middle region and a conserved thymine (-14). All 12 previously shown RpoN-controlled promoters were confirmed, including *hcp* and *flaA* (Supplementary Table S2). Forty-eight (70%) RpoN-binding peaks were found within 250-bp upstream of an open reading frame (ORF). There were seven RpoN-binding sites located inside genes and distant from the 5' end of the nearest downstream gene (Supplementary Table S2). To validate ChIP-Seq results, we tested the ChIP enrichment by qPCR. Results show at least 10-fold enrichment for all binding sites except for VCA0925, which had a 2.9- ± 0.6-fold enrichment (Supplementary Figure S2).

Transcriptome profiling of RpoN-controlled genes by RNA-Seq

The identified RpoN-binding sites may include both silent sites not involved in transcription and active promoters that drive gene expression. To differentiate these, we compared the effect of RpoN on transcriptome expression in RpoN-expressed and RpoN-deleted conditions using RNA-Seq analysis. The expression of 144 genes in 82 operons was positively controlled by RpoN (≥two-fold, $P < 0.05$) (Supplementary Table S3). These genes include >50 genes for motility and chemotaxis, all genes in the T6SS *hcp1* and *hcp2* operons, nitrogen utilization genes *glnB1*, *glnA* and *ntrB*, genes coding for formate dehydrogenase and phage shock proteins and >40 genes encoding unknown functions. Of RpoN-controlled operons, 37 possess upstream ChIP-identified RpoN-binding sites (Table 2). Thirty-five of these promoter sites are within 250 bp from the 5' end of downstream genes. It is important to note that the activity of RpoN-binding promoters requires the presence of an enhancer, and our analysis would not detect RpoN-dependent transcripts if their cognate enhancers were not expressed under the conditions tested. A large number of genes were expressed higher in the *rpoN* mutant, including many genes for metabolism (Supplementary Table S4). This is likely an indirect effect because of competition of sigma factors for binding to the limited number of RNA core polymerase (36,37). Alteration in the expression of one sigma factor results in changes in gene expression controlled by other sigma factors (37,38). For example, deletion of *rpoN* increases the expression of genes controlled by another sigma factor RpoS in *E. coli* (39).

New RpoN-dependent promoters in flagellar gene clusters

Consistent with ChIP-Seq results, all genes for motility and chemotaxis, except for *flrA*, *flgA*, *cheV-3* and *cheR-2*, showed significant difference in expression when RpoN was expressed ($P < 0.05$) (Supplementary Table S3). This is as expected because RpoN is required for motility in *V. cholerae* (18). However, the RpoN-dependence of these flagellar genes varies greatly. Flagellar genes are located in three major clusters and are regulated by RpoN, FlrA, FlrC and FliA, which form a four-tiered hierarchical regulation (20). Expression of *flrA* was independent of RpoN, whereas *flrC* and *fliA* were positively controlled by RpoN. We expect genes that require RpoN for expression to have basal expression

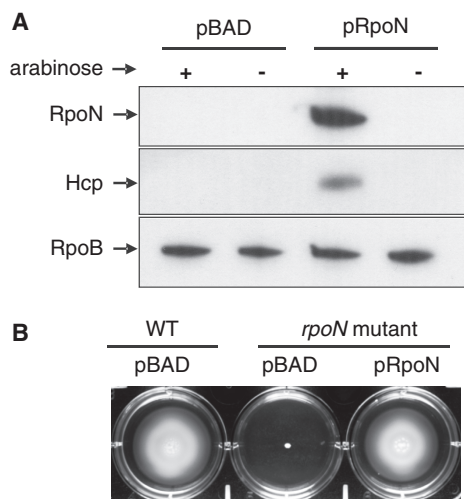


Figure 1. RpoN-3V5 complements the *rpoN* deletion mutant. The pBAD-derivative plasmid pRpoN carrying arabinose-inducible RpoN-3V5 complements two known RpoN-dependent traits in the *rpoN* mutant, Hcp expression (A) and motility (B).

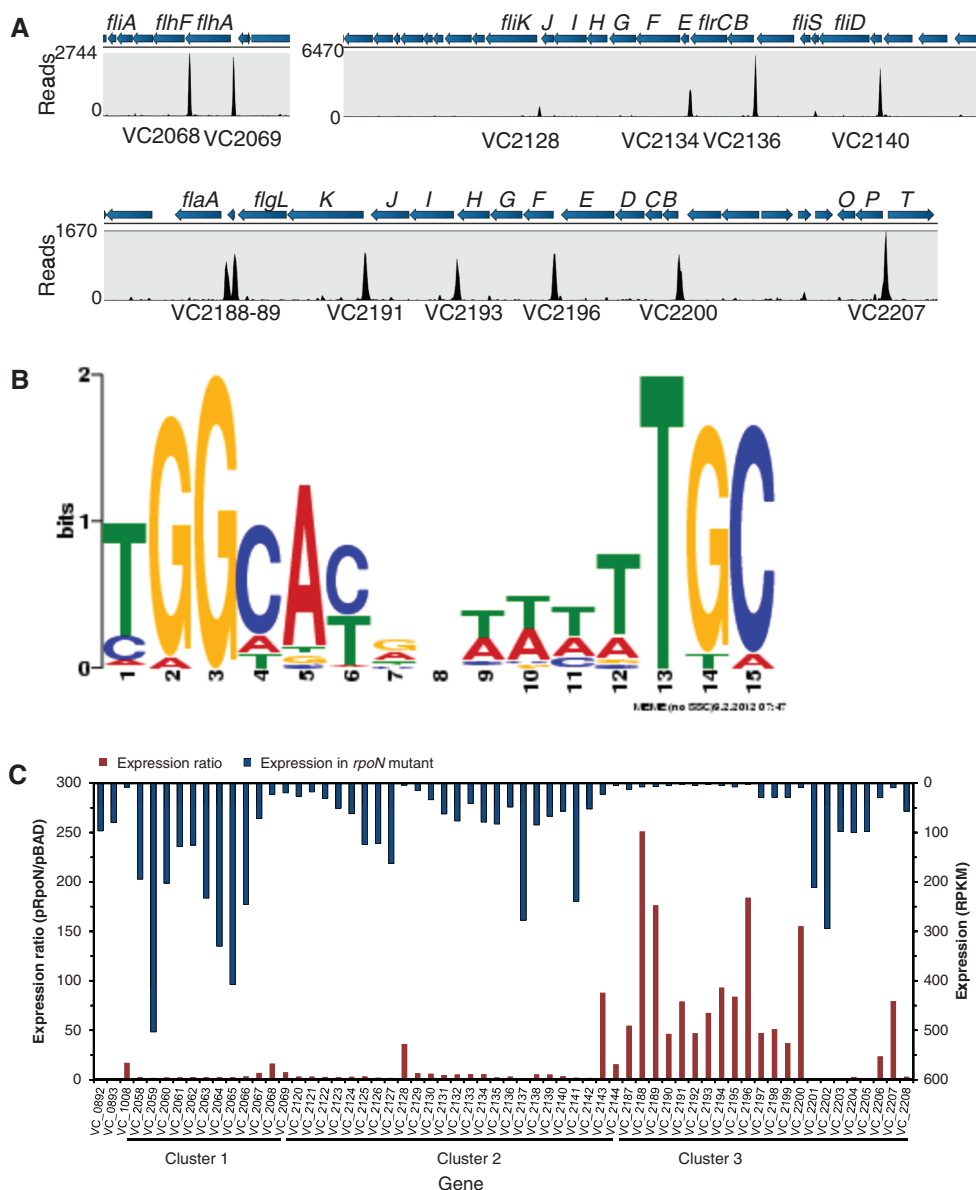


Figure 2. A sample of ChIP-Seq and RNA-Seq data covering the flagellar region and consensus RpoN-binding motif. (A) Genomic structures are shown above the peak panel. The height of each peak corresponds to the number of reads bound to the corresponding ChIP-site. (B) Motif was generated based on all ChIP-peaks using MEME program. The height of each letter represents the occurrence frequency at each location. (C) RNA-Seq data show difference in regulation of flagellar genes by RpoN. The RpoN-dependence (expression ratio) is shown at the bottom with the left axis. The absolute expression for each gene in the *rpoN* mutant is shown on the top with the right axis. Genes with high-RpoN-dependence and low-expression in the *rpoN* mutant require RpoN for expression, whereas genes with high-expression in the *rpoN* mutant likely have other promoters independent of RpoN.

levels in the *rpoN* mutant and high RpoN-dependence. These include most genes in cluster 3 (*flgBCDEFGHIJKL*, *flaA* and *flgOP*), *fliK* and *motY* (Figure 2). In contrast, most genes in the other clusters exhibited little RpoN-dependence (<4 fold) and were expressed at relatively high levels in the *rpoN* mutant, suggesting the existence of other promoters. For example, the *fliA* gene was expressed at considerable levels in the *rpoN* mutant, and the *fliA* gene in *E. coli* is known to possess both RpoD- and FliA- recognized promoters (40). In addition, *cheR-2*, a previously identified RpoN-dependent gene (20), was expressed independent of RpoN in V52.

Using ChIP-Seq and RNA-Seq, we identified new operon structures for flagellar genes (Figure 2). In addition to the previously characterized flagellar gene regulation (41), we found seven new RpoN-binding promoters for *flgF*, *flgI*, *flhF*, *fliD*, *fliK*, *motY* and *flgT* (Table 2). Two RpoN-binding peaks were identified upstream of the major flagellin gene VC2188 *flaA*: one previously known as FlrC-bound RpoN-controlled promoter upstream of VC2189 (42) and a new RpoN promoter located 144 bp upstream of VC2188 (Table 2) (Figure 2). Notably, previously identified RpoN-controlled genes *fliLMNOPQR*, *flhB*, *cheABWYZ* and

Table 2. RpoN-regulated genes identified by RNA-Seq and ChIP-Seq

Operon	Gene	Function	Fold change (pRpoN/pBAD)	P-value	ChIP-peak
T6SS					
VC1415-20	<i>hcp1/vgrG1</i>	T6SS secretion	511.1/61.9/14.8/6.4/7.0/4.7	0.001	TGGCATCCCCACTTGC
VCA0017-23	<i>hcp2/vgrG2</i>	T6SS secretion	532.5/94.1/19.0/14.5/12.7/2.8/3.8	0.001	TGGCATCCCCACTTGC
VCA0123	<i>vgrG3</i>	T6SS secretion	2.4	0.001	TGGCATTGAGTTTGC
Motility and Chemotaxis					
VC1008	<i>motY</i>	Sodium-type flagellar protein	16.9	0.001	TGGCTAGATTTTTTGC
VC1384		Putative outer membrane protein	7.6	0.001	AGGTACGAAATTTTGC
VC2068-66	<i>flhFG-flhA</i>	Flagellar biosynthesis/sigma factor FlhA	16.2/6.8/3.3	0.001	TGGAACAAATTTTTGC
VC2069	<i>flhA</i>	Flagellar biosynthesis	7.4	0.001	TGGACTGAAAATTTGC
VC2128	<i>fliK</i>	Flagellar hook-length control	36.2	0.001	TGGCTTACTTCTTGC
VC2134-29	<i>fliEFGHIJ</i>	Flagellar assembly	5.6/5.5/5.3/4.7/6.0/6.6	0.001	TGGCAGGAAAGTTGC
VC2136-35	<i>fliBC</i>	Flagellar regulator	3.2/2.3	0.001	TGGCATGACTCTTGC
VC2140-38	<i>fliD/flaI/fliS</i>	Flagellar rod/hook-associated protein	2.1/3.4/5.2/5.4	0.001	TGGCACTAAAATTTGC
VC2188	<i>flaA</i>	Flagellin core protein	251.0	0.001	TGGCACACTAATTGA
VC2189		Hypothetical protein	176.4	0.001	TGGCAGGAAAGTTGC
VC2191-90	<i>flgKL</i>	Flagellar hook-associated protein	79.0/46.2	0.001	TGGCATACATATTGC
VC2193-92	<i>flgIJ</i>	Flagellar P-ring/flagellar protein	67.6/47.6	0.001	TGGCAGGATTTTTTA
VC2196-94	<i>flgFGH</i>	Flagellar basal rod/L-ring	183.9/84.0/93.1	0.001	TGGCATGCTGCTTGC
VC2200-2197	<i>flgBCDE</i>	Basal rod protein/hook protein E	155.2/36.9/51.0/47.3	0.001	TGGTACGTAATTTGC
VC2207-06	<i>flgOP</i>	Outer membrane proteins	79.5/23.5	0.001	GGGTATAAATTTTTGC
VC2208	<i>flgT</i>	Flagellar assembly protein	2.4	0.001	TGGAACGCTCCTTGC
Regulator					
VC0606-07	<i>glnB-1</i>	Nitrogen regulatory protein P-II	32.7/14.8	0.005	TGGCAGCCCCCTTGC
VC2748	<i>ntxB</i>	Nitrogen regulation protein	2.8	0.001	CGGCAAGATTATTGC
Enzyme and biosynthesis					
VC1516-10		Formate dehydrogenase	63.9/44.6/40.7/69.4/48.1/51.6/22.3	0.001	TGGAACGCTATTTTGC
VC1519	<i>fdhD</i>	Formate dehydrogenase accessory	3.0	0.001	CGGCACCCTTTTTTGC
VC1523-27		ABC transporter and molybdopterin synthesis	5.4/5.7/3.9/2.3/2.1	0.001	TGGCATCCCATTTTGC
VC2746	<i>glnA</i>	Glutamate-ammonia ligase	3.4	0.004	TGGCAGCTTTTCGC
Unknown function					
VC1154		Hypothetical protein	3.8	0.001	TGGCACTCTAATTGC
VC1518-17		Hypothetical protein	7.5/10.9	0.001	TGGCGCAATTATTGC
VC1678-76	<i>pspABC</i>	Phage shock proteins	5.9/2.5/3.2	0.001	TGGATTTATCTTTGC
VC1699		Hypothetical protein	3.8	0.012	TGGCATCGGTTTTTGC
VC2005		Hypothetical protein	28.5	0.002	AGGCACAGCATTTGC
VCA0051-48		Hypothetical/GGDEF family protein	2.0/2.0/2.6/2.3	0.001	TGGCACAATTTATGC
VCA0105-06		Hypothetical protein	17.5/14.4	0.001	TGGAACATTAATTGC
VCA0144		immunogenic protein	4.9	0.012	TGGCATCTTCTTTGC
VCA0195		Hypothetical protein	4.6	0.002	CGGCACGATTTATTGC
VCA0284-86		Hypothetical protein	47.3/34.9/19.4	0.001	CGGCACCGATCATGA
VCA0734		Hypothetical protein	3.1	0.003	TGGCCTGTAATTTGC
VCA1016		Putative lipoprotein	4.3	0.010	TGGCAGCACTATGC

motX were lack of RpoN-recognized promoters and transcribed from other promoters (Supplementary Table S3).

Identification of a small RNA (sRNA), *flaX*, important for motility

RNA-Seq data revealed a highly expressed transcript that is downstream of *flaA* (Figure 3). We performed sequence analysis to scan the transcript region and did not identify any potential ORF with >20 codons, suggesting it is likely a small RNA. To test whether it is a true transcript, we performed northern blot analysis using sequence-specific oligo probes. Results confirmed the existence of this sRNA (named *flaX*), with an approximate size of 150 nt. We also used reverse-transcription PCR with primers specifically targeting *flaX* and its adjacent 3' end of *flaA* and found 164.2- ± 13.6-fold higher expression for *flaX*, consistent with the RNA-Seq results. We constructed a knock-out mutant of *flaX* that lacks 43 nt in the middle

and found that its motility was impaired in comparison with wild type, indicating an important role of *flaX* in motility. In addition, the impaired motility of the *flaX* mutant was complemented by expressing *flaX* in trans on a sRNA-expression vector pNM12 (30), which has no ribosomal-binding site upstream of the cloning site. This sRNA is likely conserved since it was also expressed in the *V. cholerae* El Tor biotype strain C6706 (data not shown). It is also important to note that transcription of *flaX* was also found in the *rpoN* mutant, suggesting its expression is independent of RpoN.

RpoN controls the expression of *hcp* but not genes on the T6SS cluster

Data from RNA-Seq and ChIP-Seq show that none of the T6SS genes on the main cluster was differentially expressed on RpoN induction and there was no RpoN-binding site. This is surprising, as previous data examining *Vibrio* T6SS promoter activity in *E. coli*

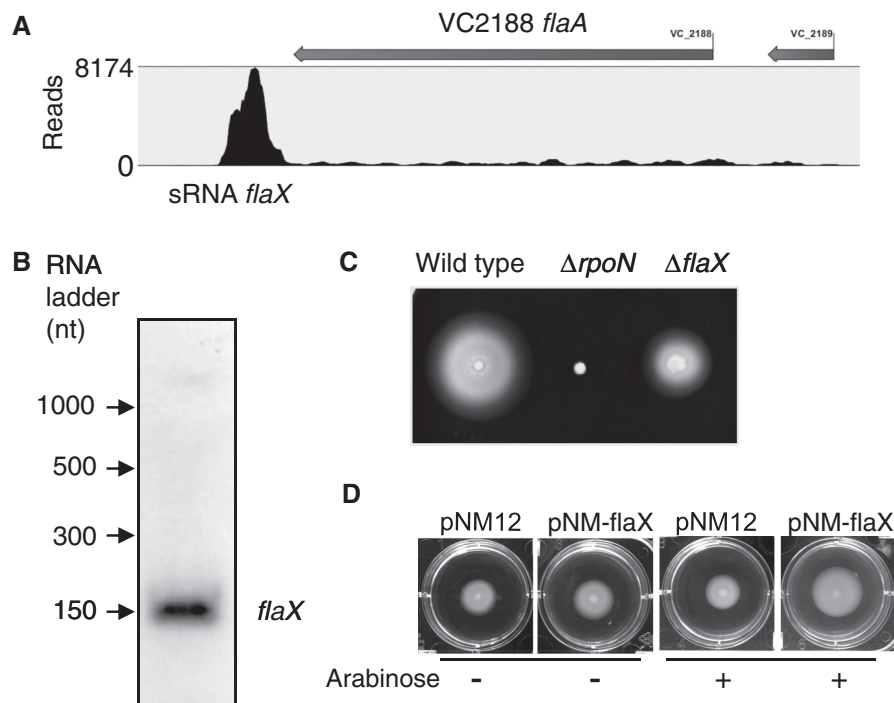


Figure 3. The new sRNA *flaX* downstream of VC2188. (A) RNA-Seq data show a substantial increase of coverage in the downstream region of *flaA*. (B) Northern blot analysis confirmed the existence of *flaX*. (C) Mutation in *flaX* attenuated motility. (D) Motility of the *flaX* mutant was complemented by expressing *flaX* in trans on a sRNA expression vector pNM12. Arabinose (0.02%) was used for inducing the expression of *flaX*.

suggest that T6SS genes on the main cluster and *hcp* were co-regulated by RpoN (21). To confirm our ChIP- and RNA-Seq data, we first compared the effect of RpoN on the expression of *hcp* and the first two genes of T6SS cluster, *vipA* (VCA0107) and *vipB* (VCA0108) (Figure 4). As expected, induction of RpoN increased Hcp levels substantially (Figure 4). Surprisingly, both VipA and VipB levels were independent of RpoN expression. In addition, the transcription levels of *hcp* and *vgrG2* were greatly induced on RpoN induction, whereas *vipA* and *vipB* levels were unaffected (Figure 4). We then tested whether RpoN binds to the promoter regions of *hcp* and *vipAB* by ChIP. There was a 90-fold enrichment for the *hcp* promoter region, whereas no difference was observed for the *vipAB* promoters and for the control gene *vgrG2* that is downstream of *hcp*, indicating that RpoN binds to the promoter of *hcp* but not *vipAB* in vivo. These results validate the RNA-Seq and ChIP-Seq data and confirm that the *hcp* operons and the major T6SS cluster are regulated differently by RpoN.

RpoN enhancer-binding protein VasH is required for the expression of *hcp* and not *vipA* or *vipB*

Because VasH is an enhancer-binding protein that activates RpoN-controlled transcription, we expect that VasH and RpoN have similar effect on the expression of T6SS genes. To test this, we compared the transcriptional levels of *hcp*, *vipA* and *vipB*, in the wild type V52 and a *vasH* deletion mutant. The expression of *hcp* was 1000-fold higher in the wild type than in the *vasH* mutant, whereas no significant change in expression was

observed for *vipA/B* in the *vasH* mutant (Figure 5). This result confirms that RpoN-VasH regulates only *hcp* operons but not the major cluster.

DISCUSSION

Development of next-generation sequencing technologies provides a revolutionary tool for studying the interaction between transcriptional factors and target DNA. In comparison with ChIP-chip and microarray, ChIP-Seq and RNA-Seq analyses provide much increased sensitivity to identify binding sites and reveal transcriptional units. However, in comparison with the large number of ChIP-Seq studies done in eukaryotes, much fewer have been performed in bacteria. Here, we present the first example of combining ChIP and RNA-Seq data to study the transcriptome and regulon structure controlled by an important transcription factor RpoN. We identified 68 RpoN-binding sites and 82 RpoN-positively regulated operons containing 144 genes. This result is comparable with previous microarray studies in which RpoN was found to control the expression of a large number of genes in the classical *V. cholerae* strain O395 (20) and El Tor O1 strain (19). Although the effect of RpoN on expression of motility genes seems to be conserved, its control on T6SS varies substantially among strains. In El Tor O1 strain, the *rpoN* mutation resulted in significant up-regulation of the T6SS locus, whereas it had little effect on *hcp* expression (19). In the classical O1 strain, the *rpoN* mutation also led to increased expression of genes on the main T6SS cluster (20). Here, we report that RpoN

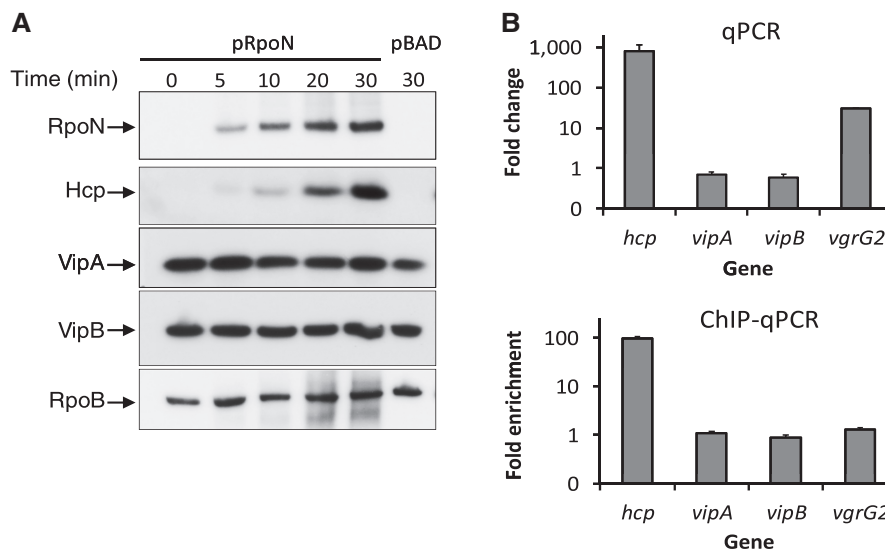


Figure 4. RpoN is required for the expression of Hcp but not VipA or VipB. (A) Protein levels of Hcp, VipA (VCA0107) and VipB (VCA0108) by western blot analysis. The *rpoN* mutant was transformed with the plasmid pRpoN or the empty vector pBAD18. Cultures were grown aerobically in LB medium at 37°C to exponential phase ($OD_{600} = 0.5$), and RpoN was induced by the addition of arabinose (0.1%) for 30 minutes. Samples were taken at different time points and protein expression was detected by western blot analysis. (B) Transcriptional levels of *hcp* and *vipAB* and ChIP-binding of their promoter regions. The *rrsA* gene encoding 16S RNA was used as an internal control sample to normalize difference in total RNA quantity among samples for qPCR. *VgrG2* is located downstream of *hcp2* and used as a control sample for ChIP assay. Monoclonal antibody to RpoN-3V5 was used for ChIP assay.

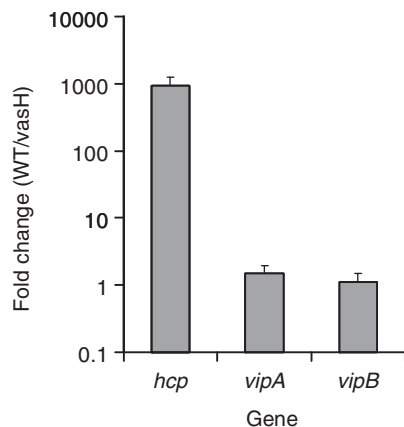


Figure 5. VasH, the enhancer-binding protein for RpoN, controls the expression of *hcp* but not the major cluster genes *vipA* and *vipB*. Relative gene expression was compared in wild type V52 and the *vasH* mutant by qPCR. The 16S ribosomal RNA gene *rrsA* was used as a control sample. RNA was extracted in exponential phase cultures $OD_{600} = 0.5$.

controls only the two *hcp* operons but not the main T6SS cluster. This adds to the notion that there is considerable genomic and genetic variation in *V. cholerae* isolates, especially in the context of virulence genes. For example, the seventh pandemic El Tor O1 strain has two unique islands, ‘*Vibrio* seventh pandemic island’ (VSP-I and VSP-II), and the RTX toxin that are not present in classical strains (43). In the case of T6SS, it is constitutively active in some *Vibrio* isolates (e.g. the O37-serotype V52) but is repressed in the seventh pandemic strain under laboratory conditions.

Of the RpoN-regulated operons, 37 operons have upstream RpoN-binding motifs indicating direct control by RpoN. The other operons lacking an RpoN-recognized promoter are likely controlled through intermediate regulators. For example, RpoN directly regulates the flagellar sigma factor FliA, which in turn regulates Class IV flagellar genes including *flaB* and *flaC* (41). In addition, many genes downstream of RpoN-binding sites were not affected by *rpoN* induction. This might be because of the presence of other promoters or the inactivity of RpoN-binding sites. The transcriptional activity of RpoN-directed promoter depends completely on cognate enhancer proteins, including their expression levels and the presence of enhancer-binding sites close to the promoter. Notably, binding of RpoN to promoter does not require enhancer binding proteins (44). Therefore, ChIP-Seq is able to detect RpoN-DNA interaction sites independent of active transcription. Indeed, we found seven binding sites that are not in close vicinity to a downstream gene. The physiological relevance of these binding sites is not clear, but it is consistent with previous results that sigma factors and RNA polymerase bind to chromosomal locations not involved in transcription. For example, RNA polymerase binds to 300 inactive transcription units (45) and a quarter of sigma 70 bound-promoters are inactive (46). Interestingly, when using the identified RpoN-binding motif to scan the genome, we found >300 potential RpoN-binding sites (data not shown), a number much larger than the reported RpoN-controlled promoter here. One predicted RpoN-binding motif is located upstream of the major T6SS cluster VCA0107, which was previously shown in *E. coli* that *E. coli* RpoN controls the activity of a plasmid-borne VCA0107

promoter and binds to the promoter region *in vitro* (21). However, this RpoN-binding motif is unlikely to be active and transcribe VCA0107 in *V. cholerae*, as the predicted transcription start site maps to the third nucleotide of the start codon of VCA0107, which would result in an out of frame translation. Indeed, our results of ChIP and expression analysis of RNA and protein levels show that RpoN does not control VCA0107 expression. How RpoN selectively binds to some but not other similar sites is still not clear. This selectivity may result from the effect of DNA topology and/or exclusive binding of other global regulators, such as IHF, Fis and H-NS. Nonetheless, this difference underscores the importance of experimental verification for *in silico* prediction of transcriptional factor binding sites.

The T6SS-encoded RpoN enhancer-binding protein, VasH, binds to the promoter of the major cluster *in vitro* (21) and is required for T6SS functions (17). However, we show that VasH, like RpoN, controls only the expression of *hcp* but not *vipAB*. This uncoupled regulation of T6SS major cluster and *hcp* operons by RpoN provides a plausible explanation for the interesting results that overexpression of *vasH* increases Hcp cellular levels but not secretion in the T6SS-inactive pandemic El Tor strain N16961 (17), as the major T6SS cluster is not subject to RpoN regulation and thus, remains non-induced. We postulate that regulation of the major T6SS cluster is the key determinant for T6SS activity. Expression of the major T6SS cluster results in not only the expression of T6SS structural genes for Hcp secretion but also the cognate RpoN enhancer protein VasH for *hcp* expression.

The flagellar gene regulatory network has been well-characterized in previous studies (20,41). Our data modify the previous model and identify seven new RpoN-controlled promoters within the large clusters of flagellar genes. Some previously characterized class II flagellar genes controlled by RpoN likely have separate promoters, as their expression does not require RpoN. We identified an sRNA *flaX* downstream of *flaA* that is required for full motility. The *in silico* analysis failed to predict a clear target for *flaX*. We are further investigating the target using an exponential enrichment pull down approach (47).

T6SS is under tight and complex control by regulators LuxO, TsrA and HapR (12), and it is recently found to be activated under high-osmolarity and low-temperature conditions (48). Although RpoN has been known as the critical regulator for T6SS function since T6SS was originally discovered, our report differentiates clearly its effect on the secreted *hcp* promoter and the main T6SS promoter. Our recent model shows that the T6SS sheath proteins VipA and VipB are in a dynamic stepwise process of forming tubular structures, contraction, disassembly and reassembly, whereas Hcp and other T6SS-dependent molecules are secreted (49). Our findings are consistent with this model that the regulation of secretion molecules differs from the components that are recycled.

SUPPLEMENTARY DATA

Supplementary Data are available at NAR Online: Supplementary Tables 1–4 and Supplementary Figures 1 and 2.

ACKNOWLEDGEMENTS

The authors thank B.D. Davies for critical reading of this manuscript. They also thank R. Bogard, W.P. Robins and M. Basler for technical assistance and the Mekalanos group for helpful discussion.

FUNDING

National Institute of Allergy and Infectious Diseases (NIAID) [AI-026289 to J.J.M.]; T.G.D. is a recipient of the Banting Postdoctoral Fellowship. Funding for open access charge: NIAID [AI-026289].

Conflict of interest statement. None declared.

REFERENCES

- Weil, A.A., Ivers, L.C. and Harris, J.B. (2012) Cholera: lessons from haiti and beyond. *Curr. Infect. Dis. Rep.*, **14**, 1–8.
- Ritchie, J.M. and Waldor, M.K. (2009) *Vibrio cholerae* interactions with the gastrointestinal tract: lessons from animal studies. *Curr. Top. Microbiol. Immunol.*, **337**, 37–59.
- Ma, A.T. and Mekalanos, J.J. (2010) In vivo actin cross-linking induced by *Vibrio cholerae* type VI secretion system is associated with intestinal inflammation. *Proc. Natl. Acad. Sci. U.S.A.*, **107**, 4365–4370.
- Pukatzki, S., Ma, A.T., Revel, A.T., Sturtevant, D. and Mekalanos, J.J. (2007) Type VI secretion system translocates a phage tail spike-like protein into target cells where it cross-links actin. *Proc. Natl. Acad. Sci. U.S.A.*, **104**, 15508–15513.
- Pukatzki, S., Ma, A.T., Sturtevant, D., Krastins, B., Sarracino, D., Nelson, W.C., Heidelberg, J.F. and Mekalanos, J.J. (2006) Identification of a conserved bacterial protein secretion system in *Vibrio cholerae* using the *Dictyostelium* host model system. *Proc. Natl. Acad. Sci. USA*, **103**, 1528–1533.
- Mougous, J.D., Cuff, M.E., Raunser, S., Shen, A., Zhou, M., Gifford, C.A., Goodman, A.L., Joachimiak, G., Ordonez, C.L., Lory, S. *et al.* (2006) A virulence locus of *Pseudomonas aeruginosa* encodes a protein secretion apparatus. *Science*, **312**, 1526–1530.
- Schwarz, S., West, T.E., Boyer, F., Chiang, W.C., Carl, M.A., Hood, R.D., Rohmer, L., Tolker-Nielsen, T., Skerrett, S.J. and Mougous, J.D. (2010) *Burkholderia* type VI secretion systems have distinct roles in eukaryotic and bacterial cell interactions. *PLoS Pathog.*, **6**, e1001068.
- Murdoch, S.L., Trunk, K., English, G., Fritsch, M.J., Pourkarimi, E. and Coulthurst, S.J. (2011) The opportunistic pathogen *Serratia marcescens* utilizes type VI secretion to target bacterial competitors. *J. Bacteriol.*, **193**, 6057–6069.
- de Pace, F., Nakazato, G., Pacheco, A., de Paiva, J.B., Sperandio, V. and da Silveira, W.D. (2010) The type VI secretion system plays a role in type I fimbria expression and pathogenesis of an avian pathogenic *Escherichia coli* strain. *Infect. Immun.*, **78**, 4990–4998.
- Pell, L.G., Kanelis, V., Donaldson, L.W., Howell, P.L. and Davidson, A.R. (2009) The phage lambda major tail protein structure reveals a common evolution for long-tailed phages and the type VI bacterial secretion system. *Proc. Natl. Acad. Sci. USA*, **106**, 4160–4165.
- Leiman, P.G., Basler, M., Ramagopal, U.A., Bonanno, J.B., Sauder, J.M., Pukatzki, S., Burley, S.K., Almo, S.C. and Mekalanos, J.J. (2009) Type VI secretion apparatus and phage tail-associated protein complexes share a common evolutionary origin. *Proc. Natl. Acad. Sci. USA*, **106**, 4154–4159.

12. Zheng, J., Shin, O.S., Cameron, D.E. and Mekalanos, J.J. (2010) Quorum sensing and a global regulator TsrA control expression of type VI secretion and virulence in *Vibrio cholerae*. *Proc. Natl. Acad. Sci. USA*, **107**, 21128–21133.
13. Ishikawa, T., Rompikuntal, P.K., Lindmark, B., Milton, D.L. and Wai, S.N. (2009) Quorum sensing regulation of the two hcp alleles in *Vibrio cholerae* O1 strains. *PLoS One*, **4**, e6734.
14. Hunt, T.P. and Magasanik, B. (1985) Transcription of *glnA* by purified *Escherichia coli* components: core RNA polymerase and the products of *glnF*, *glnG*, and *glnL*. *Proc. Natl. Acad. Sci. USA*, **82**, 8453–8457.
15. Zhao, K., Liu, M. and Burgess, R.R. (2010) Promoter and regulon analysis of nitrogen assimilation factor, sigma54, reveal alternative strategy for *E. coli* MG1655 flagellar biosynthesis. *Nucleic Acids Res.*, **38**, 1273–1283.
16. Buck, M., Gallegos, M.T., Studholme, D.J., Guo, Y. and Gralla, J.D. (2000) The bacterial enhancer-dependent sigma(54) (sigma(N)) transcription factor. *J. Bacteriol.*, **182**, 4129–4136.
17. Kitaoka, M., Miyata, S.T., Brooks, T.M., Unterwieser, D. and Pukatzki, S. (2011) VasH is a transcriptional regulator of the type VI secretion system functional in endemic and pandemic *Vibrio cholerae*. *J. Bacteriol.*, **193**, 6471–6482.
18. Klose, K.E. and Mekalanos, J.J. (1998) Distinct roles of an alternative sigma factor during both free-swimming and colonizing phases of the *Vibrio cholerae* pathogenic cycle. *Mol. Microbiol.*, **28**, 501–520.
19. Yildiz, F.H., Liu, X.S., Heydorn, A. and Schoolnik, G.K. (2004) Molecular analysis of rugosity in a *Vibrio cholerae* O1 El Tor phase variant. *Mol. Microbiol.*, **53**, 497–515.
20. Syed, K.A., Beyhan, S., Correa, N., Queen, J., Liu, J., Peng, F., Satchell, K.J., Yildiz, F. and Klose, K.E. (2009) The *Vibrio cholerae* flagellar regulatory hierarchy controls expression of virulence factors. *J. Bacteriol.*, **191**, 6555–6570.
21. Bernard, C.S., Brunet, Y.R., Gavioli, M., Llobes, R. and Cascales, E. (2011) Regulation of type VI secretion gene clusters by sigma54 and cognate enhancer binding proteins. *J. Bacteriol.*, **193**, 2158–2167.
22. Hood, R.D., Singh, P., Hsu, F., Guvener, T., Carl, M.A., Trinidad, R.R., Silverman, J.M., Ohlson, B.B., Hicks, K.G., Plemel, R.L. et al. (2010) A type VI secretion system of *Pseudomonas aeruginosa* targets a toxin to bacteria. *Cell Host. Microbe*, **7**, 25–37.
23. Russell, A.B., Hood, R.D., Bui, N.K., LeRoux, M., Vollmer, W. and Mougous, J.D. (2011) Type VI secretion delivers bacteriolytic effectors to target cells. *Nature*, **475**, 343–347.
24. MacIntyre, D.L., Miyata, S.T., Kitaoka, M. and Pukatzki, S. (2010) The *Vibrio cholerae* type VI secretion system displays antimicrobial properties. *Proc. Natl. Acad. Sci. USA*, **107**, 19520–19524.
25. Ma, A.T., McAuley, S., Pukatzki, S. and Mekalanos, J.J. (2009) Translocation of a *Vibrio cholerae* type VI secretion effector requires bacterial endocytosis by host cells. *Cell Host. Microbe*, **5**, 234–243.
26. Miyata, S.T., Kitaoka, M., Brooks, T.M., McAuley, S.B. and Pukatzki, S. (2011) *Vibrio cholerae* requires the type VI secretion system virulence factor VasX to kill *Dictyostelium discoideum*. *Infect. Immun.*, **79**, 2941–2949.
27. Davies, B.W., Bogard, R.W. and Mekalanos, J.J. (2011) Mapping the regulon of *Vibrio cholerae* ferric uptake regulator expands its known network of gene regulation. *Proc. Natl. Acad. Sci. USA*, **108**, 12467–12472.
28. Miller, V.L. and Mekalanos, J.J. (1988) A novel suicide vector and its use in construction of insertion mutations: osmoregulation of outer membrane proteins and virulence determinants in *Vibrio cholerae* requires *toxR*. *J. Bacteriol.*, **170**, 2575–2583.
29. Metcalf, W.W., Jiang, W., Daniels, L.L., Kim, S.K., Haldimann, A. and Wanner, B.L. (1996) Conditionally replicative and conjugative plasmids carrying *lacZ* alpha for cloning, mutagenesis, and allele replacement in bacteria. *Plasmid*, **35**, 1–13.
30. Majdalani, N., Cunnig, C., Sledjeski, D., Elliott, T. and Gottesman, S. (1998) DsrA RNA regulates translation of RpoS message by an anti-antisense mechanism, independent of its action as an antisilencer of transcription. *Proc. Natl. Acad. Sci. USA*, **95**, 12462–12467.
31. Guzman, L.M., Belin, D., Carson, M.J. and Beckwith, J. (1995) Tight regulation, modulation, and high-level expression by vectors containing the arabinose PBAD promoter. *J. Bacteriol.*, **177**, 4121–4130.
32. Davies, B.W., Bogard, R.W., Dupes, N.M., Gerstenfeld, T.A., Simmons, L.A. and Mekalanos, J.J. (2011) DNA damage and reactive nitrogen species are barriers to *Vibrio cholerae* colonization of the infant mouse intestine. *PLoS Pathog.*, **7**, e1001295.
33. Ji, H., Jiang, H., Ma, W., Johnson, D.S., Myers, R.M. and Wong, W.H. (2008) An integrated software system for analyzing ChIP-chip and ChIP-seq data. *Nat. Biotechnol.*, **26**, 1293–1300.
34. Bailey, T.L. and Elkan, C. (1994) Fitting a mixture model by expectation maximization to discover motifs in biopolymers. *Proc. Int. Conf. Intell. Syst. Mol. Biol.*, **2**, 28–36.
35. Mortazavi, A., Williams, B.A., McCue, K., Schaeffer, L. and Wold, B. (2008) Mapping and quantifying mammalian transcriptomes by RNA-Seq. *Nat. Methods*, **5**, 621–628.
36. Grigorova, I.L., Phleger, N.J., Mutalik, V.K. and Gross, C.A. (2006) Insights into transcriptional regulation and sigma competition from an equilibrium model of RNA polymerase binding to DNA. *Proc. Natl. Acad. Sci. USA*, **103**, 5332–5337.
37. Farewell, A., Kvint, K. and Nystrom, T. (1998) Negative regulation by RpoS: a case of sigma factor competition. *Mol. Microbiol.*, **29**, 1039–1051.
38. Jishage, M., Kvint, K., Shingler, V. and Nystrom, T. (2002) Regulation of sigma factor competition by the alarmone ppGpp. *Genes Dev.*, **16**, 1260–1270.
39. Dong, T., Yu, R. and Schellhorn, H. (2011) Antagonistic regulation of motility and transcriptome expression by RpoN and RpoS in *Escherichia coli*. *Mol. Microbiol.*, **79**, 375–386.
40. Mytelka, D.S. and Chamberlin, M.J. (1996) *Escherichia coli* *fliAZY* operon. *J. Bacteriol.*, **178**, 24–34.
41. Prouty, M.G., Correa, N.E. and Klose, K.E. (2001) The novel sigma54- and sigma28-dependent flagellar gene transcription hierarchy of *Vibrio cholerae*. *Mol. Microbiol.*, **39**, 1595–1609.
42. Correa, N.E. and Klose, K.E. (2005) Characterization of enhancer binding by the *Vibrio cholerae* flagellar regulatory protein FlrC. *J. Bacteriol.*, **187**, 3158–3170.
43. Dziejman, M., Balon, E., Boyd, D., Fraser, C.M., Heidelberg, J.F. and Mekalanos, J.J. (2002) Comparative genomic analysis of *Vibrio cholerae*: genes that correlate with cholera endemic and pandemic disease. *Proc. Natl. Acad. Sci. USA*, **99**, 1556–1561.
44. Buck, M. and Cannon, W. (1992) Specific binding of the transcription factor sigma-54 to promoter DNA. *Nature*, **358**, 422–424.
45. Herring, C.D., Raffaele, M., Allen, T.E., Kanin, E.I., Landick, R., Ansari, A.Z. and Palsson, B.O. (2005) Immobilization of *Escherichia coli* RNA polymerase and location of binding sites by use of chromatin immunoprecipitation and microarrays. *J. Bacteriol.*, **187**, 6166–6174.
46. Reppas, N.B., Wade, J.T., Church, G.M. and Struhl, K. (2006) The transition between transcriptional initiation and elongation in *E. coli* is highly variable and often rate limiting. *Mol. Cell*, **24**, 747–757.
47. Lorenz, C., von Pelchrzim, F. and Schroeder, R. (2006) Genomic systematic evolution of ligands by exponential enrichment (Genomic SELEX) for the identification of protein-binding RNAs independent of their expression levels. *Nat. Protoc.*, **1**, 2204–2212.
48. Ishikawa, T., Sabharwal, D., Broms, J., Milton, D.L., Sjostedt, A., Uhlin, B.E. and Wai, S.N. (2012) Pathoadaptive conditional regulation of the type VI secretion system in *Vibrio cholerae* O1 strains. *Infect. Immun.*, **80**, 575–584.
49. Basler, M., Pilhofer, M., Henderson, G.P., Jensen, G.J. and Mekalanos, J.J. (2012) Type VI secretion requires a dynamic contractile phage tail-like structure. *Nature*, **483**, 182–186.